Solvent Mediated Modulation of the Au-S Bond in Dithiol Molecular Junctions

Johnson Dalmieda¹, Wanzhuo Shi¹, Liang Li¹, Latha Venkataraman^{1,2*}

¹Department of Chemistry, Columbia University, 3000 Broadway, New York, NY 10027

²Department of Applied Physics, Columbia University, 500 W 120th Street, New York, NY 10027

*Email: lv2117@columbia.edu

ABSTRACT

Gold-dithiol molecular junctions have been studied both experimentally and theoretically. However, the nature of the gold-thiolate bond as it relates to the solvent has been seldom investigated. It is known that solvents can impact the electronic structure of single molecule junctions, but the correlation between the solvent and dithiol-linked single-molecule junction conductance is not well understood. We study molecular junctions formed with thiol terminated phenylenes from both 1-chloronaphthalene and 1-bromonaphthalene solutions. We find that the most probable conductance and the distribution of conductances are both affected by the solvent. First-principles calculations show that junction conductance depends on the binding configurations (adatom, atop, bridge) of the thiolate on the Au surface as has been shown previously. More importantly, we find that brominated solvents can restrict the binding of thiols to specific Au sites. This mechanism offers new insight into the effects of the solvent environment on covalent bonding in molecular junctions.

Key words: Single molecule measurements, Density Functional Theory, Scanning Tunneling Microscope-based Break Junction measurements, Thiol-gold bonding

One of the most studied classes of molecules towards their application in molecular electronics are thiols and thiolates¹ due to their popularity as a testbed for self-assembled monolayer systems² towards the fabrication of nanodevices. They have also been extensively studied, both theoretically and experimentally, at the single molecule level.³⁻⁷ In particular, the interaction between a thiolate substituent and a gold surface is of interest since forming bonds on a gold surface is rare, owing to its inertness. 8 Despite this, sulfur containing substituents can form σ-bonds on an Au-surface. In addition, the sulfur substituent also has two lone pairs. These lone pairs can interact with the gold surface to form dative bonds, which lends credence to the possibility of the formation of stronger, multi-coordinate bonds. For example, it has been shown that in solution, "chemisorption", or the formation of a covalent Au-S-R bond, is preferred over "physisorption", or the formation of a dative Au-SH-R bond, the latter of which dominate in selfassembled monolayers. 10 The multitude of binding geometries leads to single molecule junctions formed with dithiols in solution having a range of conductances, which prevents the observation of well-defined conductance values. 11, 12 However, the choice of solvent, as will be shown here, may be able to rectify the issues previously stated¹³, whether they be through physical means or through chemical modulation.

In this work, we study the effects of two different halogenated solvents, 1-chloronaphthalene (ClN) and 1-bromonaphthalene (BrN), on the conductance and binding geometries of benzene-1,4-dithiol (BDT), biphenyl-4,4'-dithiol (BPDT), and *p*-terphenyl-4,4''-dithiol (TPDT) junctions (see SI section S1 for details). We use the Scanning Tunneling Microscope-Break Junction (STM-BJ) method for these studies to collect conductance. We also employ first principles Density Functional Theory (DFT) calculations to determine the most stable binding configurations as well as their binding energies in the presence and absence of a solvent molecule. In addition, we use non-equilibrium Green's function (DFT-NEGF)¹⁵ to calculate the transmission functions for BDT in different binding configurations. We find that molecular conductance depends on the solvent environment in a manner that goes beyond solvent-induced electrostatic effects and has implications on how thiols and thiolates bind to the Au surface.

We use a custom STM-BJ setup that has been described in detail previously for single-molecule conductance measurements. ¹⁶ In this method, a gold point contact is repeatedly formed and broken between the Au tip and substrate at a bias of 100 mV in a 100 μ M solution of the target molecule. Note that we choose this concentration as lower concentrations do not yield clear conductance peaks in both solvents (see SI section S2). Conductance (I/V) is measured as a function of tip/substrate displacement and show plateaus around the conductance quantum ($G_0 = 2e^2/h$) and molecular-dependent conductance values (<1 G_0). In a typical experiment, we collect 5000 conductance traces and analyze these as one-dimensional conductance and two-dimensional conductance-displacement histograms without data selection.

In Figure 1, we show conductance histograms for all three molecules in both solvents. The histogram of BDT shows two peaks (Figure 1a); focusing on the higher conductance peak we note that the conductance is higher in ClN when compared with BrN. The same trend is also seen in the BPDT (Figure 1b) and TPDT (Figure 1c) histograms. These results are in contrast to previous work^{17, 18} which found that HOMO-conducting molecules exhibited higher conductance in

brominated solvents than chlorinated ones due to the surface bound solvents altering the Au work function.

The histograms in Figure 1 also show that the conductance peak heights and peak widths are smaller in BrN than in ClN. In addition, when we fit the conductance peaks to a Gaussian curve, the fitted curves in BrN appear to be a subset of the curves that we see in ClN. The observed differences in the shape of the histogram peaks indicate that there are changes in the probability of junction formation, ability for a junction to be elongated, as well as changes in the configurations of the junctions that do form. We also note that when comparing between the TPDT junctions formed in ClN and BrN solutions, we observe a decrease in the counts in the conductance range between $\sim 10^{0}$ - $10^{-1.5}$ G_{θ} and a sharper and better-defined 1 G_{θ} peak. These differences between measurements in ClN and BrN indicate that the origin is more chemical in nature i.e., changes in the nature of the Au-S bond, $^{19-24}$ rather than physical i.e., an electrostatic effect. $^{25-27}$ We note that the histograms in Figure 1 also have a lower conductance peak, that is most clearly visible in the measurements of BDT. We hypothesize that this is due to the formation of a dimer which could be two molecules coupled through a disulfide bridge 28 , a gold atom or through π - π stacking interactions. 29 The exact origin of this lower conductance peak and flicker noise measurements are further discussed in Section S3 in the Supplementary Information.

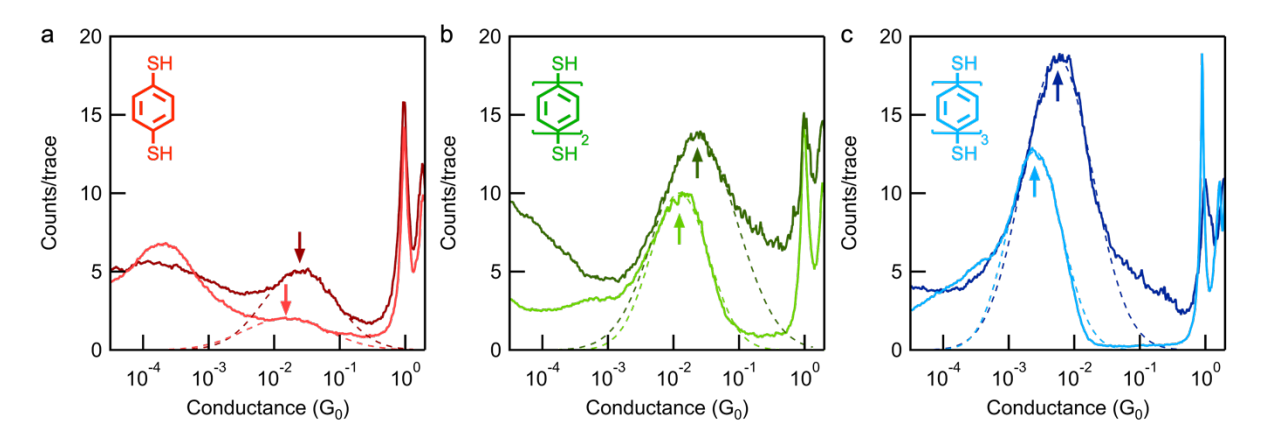


Figure 1. One-dimensional conductance histograms of a) BDT, b) BPDT, and c) TPDT in ClN (dark) and BrN (light) solution. Dashed lines are the Gaussian fit to the conductance peaks, and arrows highlight the fit maxima. Insets: Molecular structures of BDT, BPDT, and TPDT.

We must note that the 2D histograms do not contain correction factors for the snapback distance as that is not a measured parameter in our experiments. Rather, the change in junction length as the solvent is changed, regardless of snapback distance, is what we highlight here. The 2D histogram for BDT in ClN (Figure 2a) show a more sloped feature when compared to BDT in BrN (Figure 2b). This is more clearly seen in the 2D histograms for BPDT and TPDT (Figures 2c-f). Junctions formed in ClN decrease in conductance as the displacement is increased, whereas in BrN they have minimal correlation with displacement. This is an indication that changes in the binding geometry may be occurring as the junction is elongated in ClN. By contrast, in BrN, our data could indicate that binding configurations are restricted, similar to what is seen with selective linkers

such as phosphines, methyl sulfides or amines.³⁰ We can also deduce this by observing the difference in plateau lengths between junctions formed in ClN and in BrN. The longer junction plateaus present in ClN may hint at the fact that there exists a variety of junction configurations that we can observe, whereas these configurations may be limited in BrN.

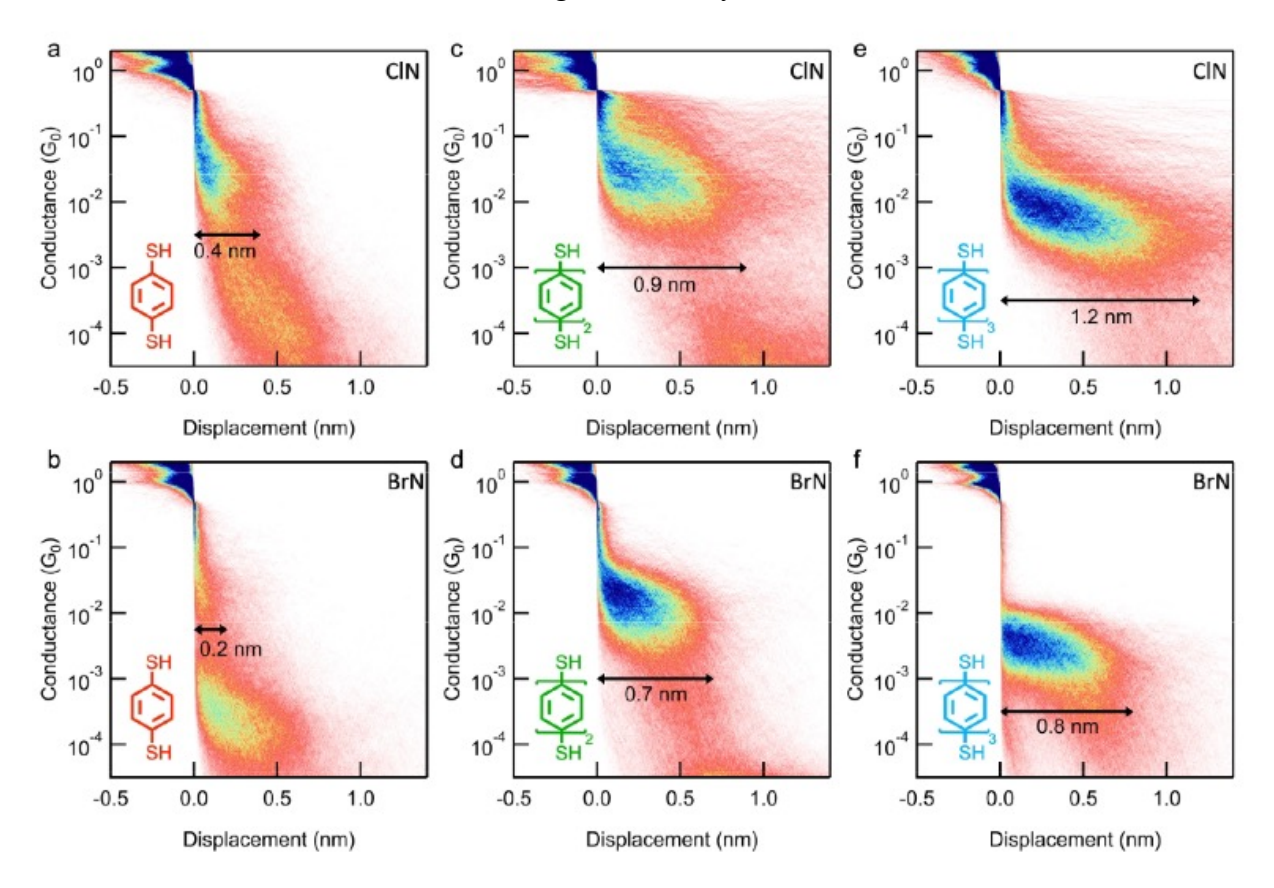


Figure 2. Two-dimensional conductance-displacement histograms. a) BDT in ClN. b) BDT in BrN. c) BPDT in ClN. d) BPDT in BrN. e) TPDT in ClN. f) TPDT in BrN. The approximate elongation length of the junction is indicated by the arrows in the histograms.

It is known that thiolates can bind to a gold surface through a single or multiple bonds to Au atoms, specifically involving singly-coordinate (adatom, atop), doubly-coordinate (bridge), and triply-coordinate (hollow) geometries.^{31, 32} To this end, we use DFT calculations to optimise the structure of the BDT on a Au tetrahedron in each of these binding mode (Figure 3a-c). We perform geometry relaxation using the Perdew-Burke-Ernzerhof³³ functional as implemented in the FHI-aims software package.^{34,35} To determine the binding energies of the four different binding motifs, we bind a BDT to a 5-layer Au tetrahedron through a covalent Au-S bond after removing the H on the thiol, and allow it to relax. We keep the Au electrode coordinates fixed and place the H at the bottom of the tetrahedron during the relaxation. The calculated binding energies for each configuration are given in Table 1. We note first that our binding energies are the energies gained by the system when the molecule (with its hydrogen) bind to gold. These are much lower than the energy required to break the Au-S bond starting for the relaxed configuration (see SI Section S4 for details). The latter number is also indicated in the table. Based on the trends in binding energy,

we find that the bridge geometry is preferred over the atop geometry on a flat Au surface consistent with previous studies.³⁶ We did not observe a stable hollow geometry, with the molecule reverting to a bridge configuration after energy minimization similar to previous work by Tachibana *et. al.*⁹ The most stable geometry is however the adatom geometry since the S is bound to an undercoordinated Au atom.

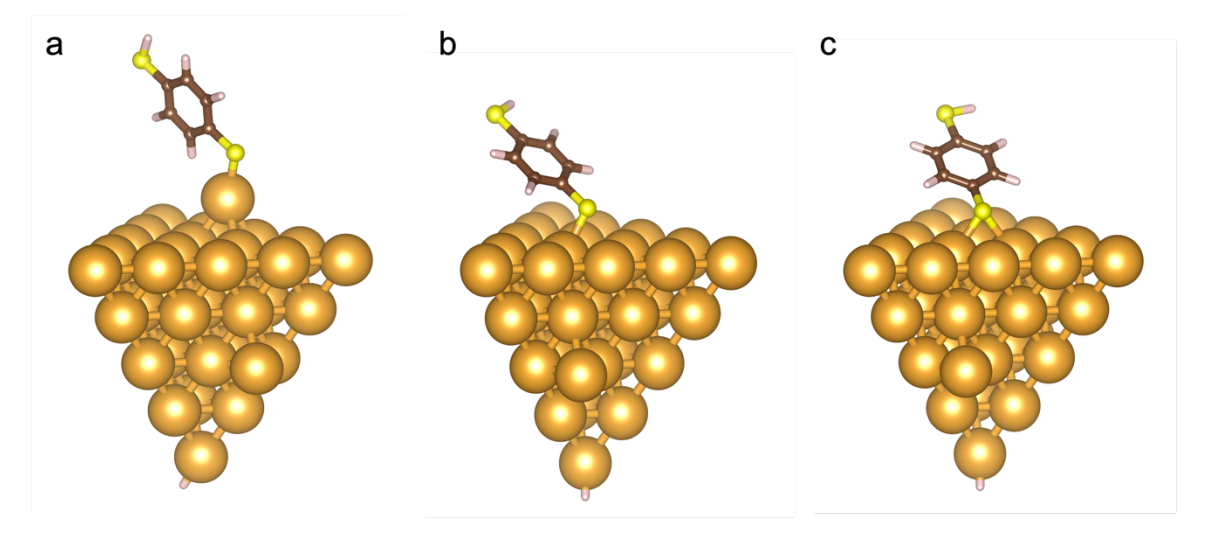


Figure 3. The optimized geometries of the Au-BDT showing different binding motifs for a) adatom, b) atop, and c) bridge configurations.

	Au-S bond distance (Å)	Au-S-C angle	Binding Energy (eV)*
Adatom	2.29	110.0°	-0.59 (-1.78)
Atop	2.46	106.0°	-0.21 (-1.40)
Bridge	2.53	112.9°	-0.36 (-1.54)

Table 1. Bond distances, bond angles, and binding energies of BDT in three different geometries attached to a 5-layer Au tetrahedron. *Values in the parentheses are the calculated Au-S bond strength).

To understand the impact of the solvents, we calculate the binding energies for the adsorption of a ClN or a BrN molecule on the Au tetrahedron (see SI Section S5 for details). We find that the binding energy of BrN on the adatom site is around 0.51 eV while that of a ClN is 0.39 eV. At room temperature, the probability that a BrN binds to an Au adatom is roughly 120 times larger than that of a ClN. Although the probability that a thiol binds to an adatom is only 24 times larger than that of BrN, the concentration of the BrN around the Au is much larger than that of the thiol (a factor of > 70000). There undercoordinated sites on the Au electrode are likely decorated with BrN increasing the probability of observing the bridge site geometry when measurements are made in BrN. In ClN however, since the ClN-Au bond is likely not strong enough to be sustained at room temperature, the probability of observing atop and adatom bound thiols becomes much more likely.

We next calculate transmission functions for BDT junctions in the three aforementioned configurations focusing on symmetric junctions (Figure 4). The transmission function was calculated using the non-equilibrium Green's function (NEGF) as implemented in the FHI-aims software package with the PBE functional.³⁷⁻³⁹ We first optimize the geometry of the molecule, then attached it to one Au_{37} tetrahedron after removing the H on the S and reoptimize the geometry freezing the Au atoms. We then construct the junction by enforcing inversion symmetry. We see in all junctions that transmission at E_F , $T(E_F)$, is dominated by the HOMO of the molecule as illustrated by the scattering state at E_F . $T(E_F)$ is the highest for the adatom and atop configurations and lower for the bridge configuration. Note that these transmission values, evaluated at E_F , are based on DFT, and have errors inherent to the method⁴⁰ and thus although trends in transmission are accurate, the magnitude is overestimated. Comparing the range of the peak in the histogram, we find that theory overestimates conductance by a factor of 3-10. The understanding we gain through the binding energy and transmission calculations indicate that in BrN, the bridge-binding geometry is preferred, and this has a lower transmission at E_F . In ClN, the solvent does not compete with the analyte in binding to Au giving a larger spread in transmissions.

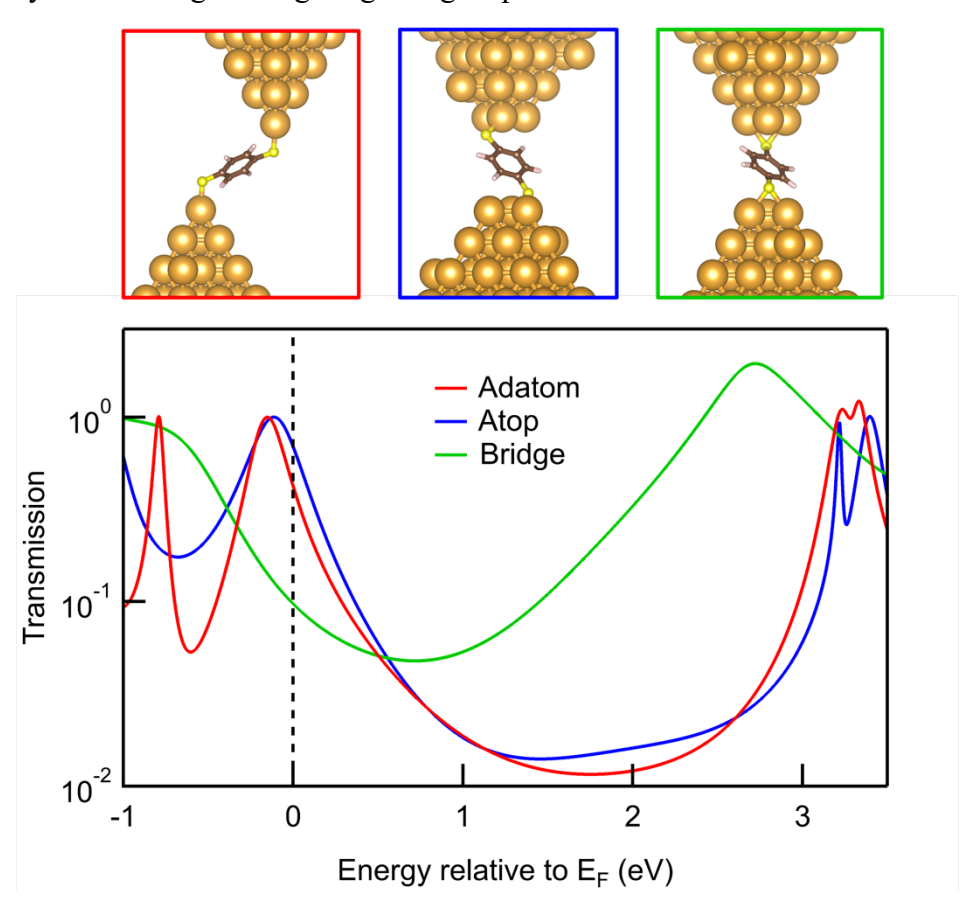


Figure 4. Transmission functions of BDT in the adatom, atop, and bridge geometries calculated for the junction structures shown.

In conclusion, BDT, BPDT, and TPDT single molecule junctions formed in BRN are seen to have lower conductance, lower pickup rates, and shorter junction lengths than what was observed in CLN. The shape and peak widths of the conductance histograms indicate that this

difference between solvents results from the nature of the Au-S bond in each solvent. DFT calculations of binding energies for BDT show a binding preference in the order of adatom>bridge>atop. The calculated transmission functions for all the binding configurations in BDT show that the conductance values for the bridge geometry is lower than that of the atop or adatom. Thus, the decrease in conductance observed in the experiments changing solvents from CLN to BRN solution can be attributed to the increased probability of observing the bridge binding mode in BRN. We have shown that the solvent environment can not only affect the molecule physically through the change in work function caused by surface dipoles as seen in previous work¹⁸, but also chemically through the changes in binding modes of linker substituents that bond to the Au electrodes.

SUPPORTING INFORMATION

Information on materials used, additional 1D conductance histograms, flicker noise analysis and discussion, discussion on binding energy calculations, solvent binding energies.

ACKNOWLEDGEMENTS

This work was supported primarily by the NSF CHE-2023568 CCI Phase I: Center for Chemistry with Electric Fields and by NSF DMR-2241180. W.S. was supported by the U.S.-Israel Binational Science Foundation Award 2020327.

AUTHOR INFORMATION

Johnson Dalmieda – <u>id3847@columbia.edu</u>

Wanzhuo Shi – ws2637@columbia.edu

Liang Li – ll3332@columbia.edu

Latha Venkataraman – <u>lv2117@columbia.edu</u>

REFERENCES

- (1) Hakkinen, H. The gold-sulfur interface at the nanoscale. *Nat. Chem.* **2012**, *4* (6), 443-455.
- (2) Dubois, L. H.; Nuzzo, R. G. Synthesis, Structure, and Properties of Model Organic Surfaces. *Ann. Rev. Phys. Chem.* **1992**, *43* (1), 437-463.
- (3) Huang, Z.; Chen, F.; Bennett, P. A.; Tao, N. Single molecule junctions formed via Au-thiol contact: stability and breakdown mechanism. *J. Am. Chem. Soc.* **2007**, *129* (43), 13225-13231.
- (4) Kim, B.; Choi, S. H.; Zhu, X. Y.; Frisbie, C. D. Molecular tunnel junctions based on piconjugated oligoacene thiols and dithiols between Ag, Au, and Pt contacts: effect of surface linking group and metal work function. *J. Am. Chem. Soc.* **2011**, *133* (49), 19864-19877.
- (5) Souza Ade, M.; Rungger, I.; Pontes, R. B.; Rocha, A. R.; da Silva, A. J.; Schwingenschloegl, U.; Sanvito, S. Stretching of BDT-gold molecular junctions: thiol or thiolate termination? *Nanoscale* **2014**, *6* (23), 14495-14507.
- (6) Stokbro, K.; Taylor, J.; Brandbyge, M.; Mozos, J. L.; Ordejón, P. Theoretical study of the nonlinear conductance of Di-thiol benzene coupled to Au(1 1 1) surfaces via thiol and thiolate bonds. *Comp. Mat. Sci.* **2003**, *27* (1-2), 151-160.

- (7) Strange, M.; Rostgaard, C.; Häkkinen, H.; Thygesen, K. S. Self-consistent GW calculations of electronic transport in thiol- and amine-linked molecular junctions. *Phys. Rev. B* **2011**, *83* (11).
- (8) Haruta, M. When Gold Is Not Noble: Catalysis by Nanoparticles. *Chem. Rec.* **2003**, *3* (2), 75-87.
- (9) Tachibana, M.; Yoshizawa, K.; Ogawa, A.; Fujimoto, H.; Hoffmann, R. Sulfur—Gold Orbital Interactions which Determine the Structure of Alkanethiolate/Au(111) Self-Assembled Monolayer Systems. *J. Phys. Chem. B* **2002**, *106* (49), 12727-12736.
- (10) Inkpen, M. S.; Liu, Z. F.; Li, H.; Campos, L. M.; Neaton, J. B.; Venkataraman, L. Non-chemisorbed gold-sulfur binding prevails in self-assembled monolayers. *Nat. Chem.* **2019**, *11* (4), 351-358.
- (11) Pontes, R. B.; Rocha, A. R.; Sanvito, S.; Fazzio, A.; da Silva, A. J. Ab initio calculations of structural evolution and conductance of benzene-1,4-dithiol on gold leads. *ACS Nano* **2011**, *5* (2), 795-804.
- (12) Komoto, Y.; Fujii, S.; Nakamura, H.; Tada, T.; Nishino, T.; Kiguchi, M. Resolving metal-molecule interfaces at single-molecule junctions. *Sci. Rep.* **2016**, *6*, 26606.
- (13) Venkataraman, L.; Klare, J. E.; Tam, I. W.; Nuckolls, C.; Hybertsen, M. S.; Steigerwald, M. L. Single-molecule circuits with well-defined molecular conductance. *Nano Lett.* **2006**, *6* (3), 458-462.
- (14) Adak, O.; Rosenthal, E.; Meisner, J.; Andrade, E. F.; Pasupathy, A. N.; Nuckolls, C.; Hybertsen, M. S.; Venkataraman, L. Flicker Noise as a Probe of Electronic Interaction at Metal-Single Molecule Interfaces. *Nano Lett.* **2015**, *15* (6), 4143-4149.
- (15) Datta, S. Electronic Transport in Mesoscopic Systems; Cambridge University Press, 2013.
- (16) Xu, B.; Tao, N. J. Measurement of single-molecule resistance by repeated formation of molecular junctions. *Science* **2003**, *301* (5637), 1221-1223.
- (17) Nakashima, S.; Takahashi, Y.; Kiguchi, M. Effect of the environment on the electrical conductance of the single benzene-1,4-diamine molecule junction. *Beilstein J. Nanotechnol.* **2011**, 2, 755-759.
- (18) Fatemi, V.; Kamenetska, M.; Neaton, J. B.; Venkataraman, L. Environmental control of single-molecule junction transport. *Nano Lett.* **2011**, *11* (5), 1988-1992.
- (19) Frenking, G.; Fau, S.; Marchand, C. M.; Grützmacher, H. The π -Donor Ability of the Halogens in Cations and Neutral Molecules. A Theoretical Study of AX^{3+} , AH_2X^+ , YX_3 , and YH_2X (A = C, Si, Ge, Sn, Pb; Y = B, Al, Ga, In, Tl; X = F, Cl, Br, I). *J. Am. Chem. Soc.* **1997**, *119* (28), 6648-6655.
- (20) Desiraju, G. R.; Ho, P. S.; Kloo, L.; Legon, A. C.; Marquardt, R.; Metrangolo, P.; Politzer, P.; Resnati, G.; Rissanen, K. Definition of the halogen bond (IUPAC Recommendations
- 2013). Pure App. Chem. 2013, 85 (8), 1711-1713.
- (21) Kellett, C. W.; Kennepohl, P.; Berlinguette, C. P. pi covalency in the halogen bond. *Nat. Commun.* **2020**, *11* (1), 3310.
- (22) Hassel, O. Structural aspects of interatomic charge-transfer bonding. *Science* **1970**, *170* (3957), 497-502.
- (23) Bauer, J.; Braunschweig, H.; Brenner, P.; Kraft, K.; Radacki, K.; Schwab, K. Late-transition-metal complexes as tunable Lewis bases. *Chem.* **2010**, *16* (39), 11985-11992.
- (24) Aliyarova, I. S.; Tupikina, E. Y.; Ivanov, D. M.; Kukushkin, V. Y. Metal-Involving Halogen Bonding Including Gold(I) as a Nucleophilic Partner. The Case of Isomorphic Dichloroaurate(I). Halomethane Cocrystals. *Inorg. Chem.* **2022**, *61* (5), 2558-2567.

- (25) Leary, E.; Hobenreich, H.; Higgins, S. J.; van Zalinge, H.; Haiss, W.; Nichols, R. J.; Finch, C. M.; Grace, I.; Lambert, C. J.; McGrath, R.; et al. Single-molecule solvation-shell sensing. *Phys. Rev. Lett.* **2009**, *102* (8), 086801.
- (26) Lee, H. J.; Jamison, A. C.; Lee, T. R. Surface Dipoles: A Growing Body of Evidence Supports Their Impact and Importance. *Acc. Chem. Res.* **2015**, *48* (12), 3007-3015.
- (27) Kahn, A.; Koch, N.; Gao, W. Electronic structure and electrical properties of interfaces between metals and π -conjugated molecular films. *J. Polym. Sci. B Polym. Phys.* **2003**, *41* (21), 2529-2548.
- (28) Zheng, J.; Liu, J.; Zhuo, Y.; Li, R.; Jin, X.; Yang, Y.; Chen, Z. B.; Shi, J.; Xiao, Z.; Hong, W.; et al. Electrical and SERS detection of disulfide-mediated dimerization in single-molecule benzene-1,4-dithiol junctions. *Chem Sci* **2018**, *9* (22), 5033-5038.
- (29) Tang, Y.; Zhou, Y.; Zhou, D.; Chen, Y.; Xiao, Z.; Shi, J.; Liu, J.; Hong, W. Electric Field-Induced Assembly in Single-Stacking Terphenyl Junctions. *J. Am. Chem. Soc.* **2020**, *142* (45), 19101-19109.
- (30) Park, Y. S.; Whalley, A. C.; Kamenetska, M.; Steigerwald, M. L.; Hybertsen, M. S.; Nuckolls, C.; Venkataraman, L. Contact chemistry and single-molecule conductance: a comparison of phosphines, methyl sulfides, and amines. *J. Am. Chem. Soc.* **2007**, *129* (51), 15768-15769.
- (31) Kaneko, S.; Murai, D.; Marques-Gonzalez, S.; Nakamura, H.; Komoto, Y.; Fujii, S.; Nishino, T.; Ikeda, K.; Tsukagoshi, K.; Kiguchi, M. Site-Selection in Single-Molecule Junction for Highly Reproducible Molecular Electronics. *J. Am. Chem. Soc.* **2016**, *138* (4), 1294-1300.
- (32) Kaneko, S.; Montes, E.; Suzuki, S.; Fujii, S.; Nishino, T.; Tsukagoshi, K.; Ikeda, K.; Kano, H.; Nakamura, H.; Vazquez, H.; et al. Identifying the molecular adsorption site of a single molecule junction through combined Raman and conductance studies. *Chem Sci* **2019**, *10* (25), 6261-6269.
- (33) Perdew, J. P.; Burke, K.; Ernzerhof, M. Generalized Gradient Approximation Made Simple [Phys. Rev. Lett. 77, 3865 (1996)]. *Phys. Rev. Lett.* **1997**, 78 (7), 1396-1396.
- (34) Blum, V.; Gehrke, R.; Hanke, F.; Havu, P.; Havu, V.; Ren, X.; Reuter, K.; Scheffler, M. Ab initio molecular simulations with numeric atom-centered orbitals. *Comp. Phys. Comm.* **2009**, *180* (11), 2175-2196.
- (35) Havu, V.; Blum, V.; Havu, P.; Scheffler, M. Efficient integration for all-electron electronic structure calculation using numeric basis functions. *J. Comp. Phys.* **2009**, *228* (22), 8367-8379.
- (36) Wang, H.; Leng, Y. Gold/Benzenedithiolate/Gold Molecular Junction: A Driven Dynamics Simulation on Structural Evolution and Breaking Force under Pulling. *J. Phys. Chem. C* **2015**, *119* (27), 15216-15223.
- (37) Arnold, A.; Weigend, F.; Evers, F. Quantum chemistry calculations for molecules coupled to reservoirs: formalism, implementation, and application to benzenedithiol. *J. Chem. Phys.* **2007**, *126* (17), 174101.
- (38) Wilhelm, J.; Walz, M.; Stendel, M.; Bagrets, A.; Evers, F. Ab initio simulations of scanning-tunneling-microscope images with embedding techniques and application to C58-dimers on Au(111). *Phys. Chem. Chem. Phys.* **2013**, *15* (18), 6684-6690. DOI: 10.1039/c3cp44286a .
- (39) Bagrets, A. Spin-Polarized Electron Transport Across Metal-Organic Molecules: A Density Functional Theory Approach. *J. Chem. The. Comput.* **2013**, *9* (6), 2801-2815.
- (40) Becke, A. D. Perspective: Fifty years of density-functional theory in chemical physics. *J. Chem. Phys.* **2014**, *140* (18), 18A301.